

Geochemical Structure of Base-Metal Filling Veins and Parameters of Hydrothermal Ore Formation

M. V. Borisov, D. A. Bychkov, and Yu. V. Shvarov

Division of Geology, Moscow State University, Vorob'evy gory, Moscow, 119992 Russia

E-mail: borisov@geol.msu.ru

Received March 3, 2005

Abstract—The aim of this study was to determine at which parameters hydrothermal systems generate rich veins with bulk sphalerite contents of 30% and local concentrations in vein cross sections up to 60–70% and more. Such contents were found in the vein bodies of the Dzhimi deposit in the Sadon ore district, North Osetiya. For this purpose, we examined the thermodynamic models of the formation of base-metal filling veins. Ore-bearing fluids are formed in the root part of the hydrothermal system by the interaction of barren solutions with the host rocks (granites), which contain background contents of ore elements. The thermodynamic simulations were conducted for the system H–O–K–Na–Ca–Mg–Al–Si–Fe–C–Cl–S–Zn–Pb–Cu, which is described by 54 minerals of constant and variable composition and 78 aqueous species. The calculations for the mobilization zone were carried out for the temperature range of 360–440°C (through 10°C) and pressures of 600–1200 bar (with a 100 bar step). At each of the indicated temperature and pressure values, 100 waves (portions) of primary barren solution were subsequently passed through the granites. More than 20 complete models of the formation of filling veins (each model involving from 1000 to 1300 calculations) were constructed for individual *T-P* points in the mobilization zone, which was modeled by a sequence of multiwave step flowing reactors with a step of 10°C from 350–420 to 100°C at a constant pressure within the range of 600–1100 bar. We studied the effect of different background contents of Zn and Pb in granites on the efficiency of mobilization and ore formation and compared the relations in the naturally occurring distribution of ore elements along the continuous cross sections through Pb–Zn veins with the results of thermodynamic simulation. It was established that ore bodies with indicated bulk and local cross sectional contents of sphalerite could be formed in a narrow range of conditions in the mobilization zone (410–440°C and 900–1200 bar) and elevated background contents of Zn (more than 0.007 wt %) in the host granite. The maximum sphalerite contents (bulk and local in vein cross sections) are achieved up to the model veins within the temperature range of 150–200°C.

DOI: 10.1134/S0016702906110048

INTRODUCTION

The aim of this work was to reconstruct the conditions, processes, and mechanisms of the formation of hydrothermal vein deposits. The general methodical approach combined the geochemical study of the detailed distribution structures of elements in primary halos and veins (with continuous sampling conducted with a step of 2–5 cm) and thermodynamic computer simulation of the processes that occurred in the hydrothermal system. The simulation results were verified by their comparison with independent data, which were not included in the model. These are data on vein Pb–Zn deposits of the Sadon base-metal district of North Osetiya (Kholst, Arkhon, Verkhniy Zgid, Dzhimi), which we studied in field. Our work pioneered in developing a quantitative physicochemical model for deposits of this type.

GEOLOGICAL BACKGROUND AND FORMULATION OF THE SIMULATION PROBLEM

The main goal of this work was to determine the parameters of hydrothermal systems, which generated

rich veins with bulk Zn contents of more than 20 wt % (or sphalerite $\geq 30\%$) and local Zn contents in the vein cross sections of ≥ 40 wt % (ZnS up to 60–70%).

The formulation of the problem was based on the geochemical study of the ore bodies of the Dzhimi deposit. The newly invented features of the field technique involved the detailed continuous sampling across vein ore bodies. Large oriented monoliths of vein material (one or several) representing the complete cross-section of the vein were taken at mine workings. At the field base, the monoliths were cut by a stone-cutter into sequences individual of samples >1 –3 kg in mass. Four vein bodies from two deposits of the Sadon district were sampled along cross sections with a sampling step of 2–4 cm to study the distribution of Fe, Zn, Pb, Cu, Cd, Sb, As, Ag, and Mn. The data obtained for main elements (Fe, Zn, Pb, and Cu) are presented in the table and as plots for discussing the results. The high bulk Zn contents in the vein bodies of the Dzhimi deposit (Bozang ore zone) ubiquitously coincide with its local maximums in individual sampling intervals across vein section (up to the formation of bands of almost monomineral sphalerite).

Bulk contents (wt %) of elements in the vein bodies

Vein (level, deposit)	Thickness, cm	Number of samples (step)	Fe	Pb	Zn	Cu
Malaya (level 0, Arkhon)	24	8 (3 cm)	16.4 (7–28.6)*	4.5 (2.7–9.4)	4.1 (1.3–8.1)	0.16 (0.03–0.7)
Tsentrāl'naya Bozang (adit 47, Dzhimi)	≥60	14 (4 cm)	17.1 (9.5–20.6)	4.2 (1.6–10.3)	18.7 (11.8–40)	0.22 (0.09–0.6)
Zapadnaya-3 apophysis–Bozang (adit 47, crosscut 22, Dzhimi)	16	8 (2 cm)	8.7 (6.8–12.2)	0.5 (0.1–1.6)	17.6 (3.7–41.2)	0.11 (0.05–0.2)
Zapadnaya-3 apophysis–Bozang (adit 47, splitting 5, Dzhimi)	24	12 (2 cm)	9.7 (8.4–14.3)	1.0 (0.03–2.7)	23.8 (11.8–37.3)	0.19 (0.08–0.3)

* Numbers in parentheses show the scatter of elements in discrete sampling intervals along the cross section of the vein (minimum–maximum, wt %).

As is seen in the table, the Tsentrāl'naya vein of the Bozang ore zone (Severnyi drift, adit 47, Dzhimi) and apophyses striking parallel to the main vein at a distance of up to a few meters or at an acute angle have bulk Zn contents from 17.6 to 23.8 %. The high Zn contents are typical of the veins of the Bozang ore zone. For example, according to data of GRP "Tsvetmetrazvedka," Vladikavkaz, the bulk contents over several sampling intervals along the Osnovnaya vein (step of 5 m, Osnovnoi drift, adit 47, Dzhimi), vary from 10–12 to 30 %. Such high Zn contents rarely occur in most veins presently developed at other deposits of the district. Twelve vein bodies were previously sampled at the Verkhni Zgid (0–14 levels), Arkhon (0–7 levels), Kholst (3–7 levels) deposits at more than 30 sites for bulk Zn, Pb, and Cu. Only two sites yielded Zn contents close to those in the Bozang ore zone: Gatsirovskaya vein (Zn = 16.4% at Pb up to 1 %, level 6, Zgid) and Promezhutochnaya vein (Zn = 13.4% at Pb = 4.4%, 0 level, Arkhon). The rare occurrence of rich veins at other deposits of the district is related to their long mining history, when high-grade ores were the first-priority mining targets. The prospecting at the Dzhimi deposit is in progress, and rich ore bodies are available for study. Galena and sphalerite are unevenly distributed in the veins of the Sadon deposits, showing wide variations, from trace to 19–20% (occasionally more, up to 40%) with average Pb and Zn contents in grouped ore samples equal to 4–5% [1]. This indicates that rich ores are also present at other deposits of the district, i.e., their formation was not occasional but typical of this district.

The formation of vein portions rich in an ore component or ore columns is typical of many deposits. Their genesis is typically explained by diverse structural factors: the unequal opening of the vein cavity during intra-ore deformations, a change in the geometry and bedding of ore-controlling structures, the junctions or intersections of main ore-bearing fracture with subsidiary ones, the presence of diverse seals, and others [2]. However, much less attention was paid to the parameters of the hydrothermal system itself, which

also could be of great importance for the formation of high-grade ores: concentrations of valuable components in the ore-forming hydrothermal solution and the causes of their formation, the temperature and pressure of the initiation of the hydrothermal solutions, the evolution of metal content in the solutions, rock/water interactions, and others. These parameters of hydrothermal systems, largely inaccessible for direct study, will be considered in this work.

GEOLOGICAL MODEL OF HYDROTHERMAL SYSTEM

Most steeply dipping veins of the Sadon ore district are localized within Middle–Late Paleozoic granites. The granite massif is located in the near-axial part of the Sadon–Unal anticline. The main rock-forming minerals are quartz (25–45%), plagioclase, typically oligoclase (25–40%), orthoclase, microcline (20–25%), muscovite, and biotite (< 7%). The granites are mainly medium-grained and are rimmed by a wide band of tuffs, fine-grained clastic tuffobrecias, andesite–dacite porphyritic lavas, and sedimentary rocks of Jurassic age (J_1 – J_2). The ores are mainly hosted in granites and more rarely in porphyritic flows [3]. The generally accepted concepts suggest that the sublatitudinal deep-seated Sadon–Unal normal fault bounding the vein deposits in the south served as an ore conduit. All main deposits are controlled by auxiliary shear and detachment fractures of general NW and NE strike, which are confined to the lying wall of the normal fault. The ores were formed in the pre-Callovian time (J_2). All veins dip subvertically and have a thickness from 0.1 to 5 m or more. The veins were mined to a depth of >1100 m (Verkhni Zgid) downdip and for more than 800 m along the strike. The ores are made up of galena, sphalerite, pyrite, chalcopyrite, and pyrrhotite. The host granites around the veins were silicified, chloritized, sericitized, and carbonatized.

In the previous works [4–6], the following geological model was proposed. Mineralized waters circulated

in the Sadon–Unal fault before the deposition of the ore mineralization. The emplacement of gabbrodiabase and andesite–dacite stocks and dikes in the Middle Jurassic and intense tectonic motions formed necessary prerequisites for the initiation of the hydrothermal process: intrusions provided the required heat, while shear and detachment fractures created a zone of shattered rocks.¹ The heated solutions of the Sadon–Unal normal fault penetrated through permeable zone in the shattered Paleozoic granites and produced a mobilization zone of diverse components, including metals and sulfide sulfur. The ore-bearing solutions from the mobilization zone ascended along steep ore-controlling fissures (Fig. 1). The heat exchange with the colder host rocks and the heat loss owing to local heterogeneization during gradual cooling of the ore-bearing solutions led to the formation of base-metal filling veins and aureoles around them. Such a general scheme is confirmed by the Pb isotope composition of the ores and granites [7] and by the leaching aureoles of K, Rb, W, and other elements [8].

Unlike most deposits of the district, the ores of the Dzhimi deposit are localized in amphibolites and crystalline schists of the Upper Proterozoic–Lower Paleozoic Buron Formation. The Paleozoic granites are underlain by the Buron formation and separated from them by low-angle faults. Therefore, the mobilization zone at this deposit is located in granites.

Available data on fluid inclusions [3, 9, 10] showed that veins were formed in the district at 415–65°C and 2.3–0.11 kbar.

Updip the vein bodies, the gradients can reach 35–40°C and 250 bar per 100 m. The productive quartz–galena–sphalerite assemblage was formed within 345–120°C. The mineral-forming hydrothermal solutions were chloride–carbonate in composition (< 50% chlorides). The total salinity is a few percents (no more than 20%) of NaCl equiv. It was noted [10] that hydrothermal activity in the first structural level (Precambrian metamorphic rocks, Paleozoic granites, and Lower Jurassic volcanic rocks) produced abundant high-temperature (<415–370°C), mainly pneumatolitic–hydrothermal deposits of the earlier quartz–pyrite stage. They are confined to the junction zone of the Sadon–Unal fault with lower-order diagonal structures. The paleodepth at which the deposits of the lower level were formed was 2.5–3 km and more [3]. The pressure close to the lithostatic value at this depth should be equal to 1 kbar.

STRUCTURE OF THE THERMODYNAMIC MODELS AND SIMULATION TECHNIQUE

The mobilization zone of ore components (root zone of the hydrothermal system) was represented by a flow-

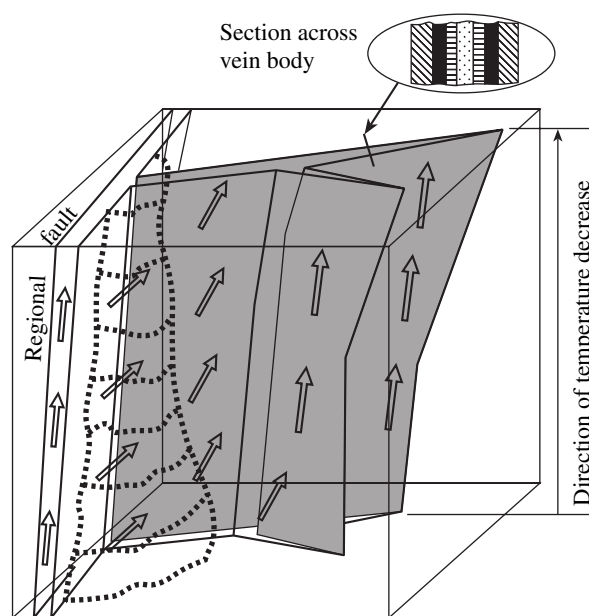


Fig. 1. Generalized scheme of a hydrothermal system. (1) Mobilization zone of ore components; (2) contact of the host rocks and fissured conduit in which an ore vein is formed; (3) percolation direction of the hydrothermal solution (from a regional fault through the mobilization zone into the fissured conduit); (4) junction of a deep-seated fault and the fissured conduit; (5–8) idealized mineral zoning of the vein at the level of productive Pb–Zn mineralization: (5) early quartz + pyrite + sphalerite ± galena assemblage; (6) quartz + sphalerite ± pyrite ± galena ± chalcopyrite assemblage (often “layers” have practically monomineral composition); (7) quartz + galena + chalcopyrite assemblage; (8) quartz core of the vein.

through reactor with a specified constant amount of unaltered granite, which contained background concentrations of Zn, Pb, and Cu. A certain amount of primary barren solution (1 kg of H₂O with dissolved CO₂ and salts) was introduced into the reactor and interacted with the granite. The rock was altered, and the newly formed equilibrium solution is regarded as the initial solution. The number of the portions or waves (below designated as W) of hydrothermal solutions can be regarded as a relative time scale. Steeply dipping fissures drained the mobilization zone to maintain the ascending movement of the ore-bearing solutions (Fig. 1). This movement is described by the system of subsequent step flow-through reactors, representing the space of the future vein body. The number of these reactors was varied depending on the temperature in the mobilization zone (from 25 to 33 in our models). The first reactor (vein inlet from below) had a temperature 20°C lower than the temperature of the mobilization zone. In each subsequent reactor, the temperature is 10°C lower than in the previous one. The last reactor (upper termination of the vein) has a temperature of

¹ The low-density zone is understood here as a zone of any strong deformations in the rocks: fissuring, fragmentation, mylonitization, and others.

100°C. Waves (portions) of solution from the mobilization zone successively passed through all reactors describing the vein. Since thermodynamic equilibrium is achieved in each reactor, solid phases precipitating during cooling remain in the reactor, and the equilibrium solution is transferred to the next reactor updip the vein. The pressure in the mobilization zone and vein is taken to be constant.

Modern methods of thermodynamic simulation (HCh package) make it possible to estimate the bulk content of minerals in and the internal structure of the vein throughout the entire interval updip the vein body. However, no data are available from the literature on the relations and tendencies in the distribution of elements in continuous cross-sections of vein bodies. Such investigations have been recently performed by us (table and plots presented during discussion) and were used for comparison with our simulation results.

Two groups of models were considered in this paper. They determined the compositional variations in the initial ore-forming solutions depending on conditions in the mobilization zone and the established correlation between mineral proportions in ore veins and conditions in the zones of mobilization and ore deposition.

The models of the first group simulating the mobilization zone, determined the compositions of ore-forming solution depending on four parameters: T , P , background content of ore elements in the host rocks, and rock/water ratio. The calculations were accomplished within the temperature range of 360–440°C (with a step of 10°C) and the pressure range of 600–1200 bar (with a step of 100 bar), i.e., at 63 individual points with different T and P parameters.

Granite from the Kholst deposit was taken as the starting host rock: SiO₂ 71.75, Al₂O₃ 13.98, Fe₂O₃ 0.105, FeO 2.333, Fe (pyrite) 0.0525, MgO 0.66, CaO 0.98, Na₂O 3.0, K₂O 4.965, H₂O 1.612, S (pyrite) 0.06 wt % [5, 6]. The background contents of ore elements in the granite were taken to be as follows: normal contents (f_0) of Zn 0.004, Pb 0.003, Cu 0.002 wt %, moderate (f_1) contents of Zn 0.007, Pb 0.006, Cu 0.002 wt %; elevated (f_2) contents of Zn 0.01, Pb 0.006, Cu 0.002 wt %. In the starting composition, metals were given in the form of oxides and in moles. For instance, 5, 10, and 15 × 10⁻⁴ mol Zn per 1 kg rock correspond, respectively, to f_0 , f_1 , and f_2 background contents, i.e., two-fold and three-fold contents are considered. The range in the background contents of Zn and Pb was determined from numerous analyses of granite at a large distance from orebodies.

At each T - P point, calculations were conducted for 10, 20, 30–40, and 100 kg granite interacting with 40–100 waves (portions) of the primary solution. The primary solution consisted of 0.5 m H₂CO₃, 1.0 m NaCl, and 0.1 m HCl. Hence, each portion of the primary solution interacting with rock contains 1 kg of water and the aforementioned amounts of H₂CO₃ and HCl. The calculations with different rock/water ratios were

conducted to decrease the step of the continuous process describing the reactions in the water–rock system. This allows us to avoid skipping in calculating the conditions of the appearance and stability fields of definite mineral assemblages.

In the models of the second group simulating formation of filling veins, the calculations were carried out not for the whole range of the T - P conditions in the models of the first group but only for selected solutions at specified T - P parameters. The starting conditions were determined by comparing the data on the mobilization zone with those simulated for the vein (bulk contents of metals, mainly Zn, and its maximum contents in the cross-section of the model vein). Each model involved from 1000 to 1300 calculated equilibria in the considered system, (mobilization zone as the zero reactor; the vein is described by 25–33 reactors, which were passed by 30–40 solution waves). Each reactor corresponds to a certain depth level in the vertical section of the vein or to certain isothermal temperature range. Twenty-one models were calculated.

The formation of filling veins was simulated in compliance with the layer mechanism, the leading mechanism in the formation of naturally occurring ore bodies [5–6, 11–14]. The layer mechanism implies that the minerals forming from each solution portion do not react with successive portions. According to the layer mechanism, the zero layer of minerals (closest to the vein contact) is formed from the solutions of wave 0, and, respectively, “layer” 20 is produced by solutions wave 20, etc. (the central parts of the veins during symmetrical growth from the two boundaries of fissur conduit). This internal structure of the mineral distribution in the cross sections of the simulated veins will be used in the results below.

Thermodynamic calculations were made with HCh package (version 3.7, author Yu. V. Shvarov), which includes the UNITHERM thermodynamic database [15, 16]. All thermodynamic data are the same as in the papers [5, 6]. The system is described by 15 independent components: H, O, K, Na, Ca, Mg, Al, Si, Fe, C, Cl, S, Zn, Pb, Cu. The model aqueous solution contains 78 species, including hydrosulfide, chloride, carbonate, and hydrocomplexes of ore elements. The list of possible minerals includes 54 solid phases, 4 ideal multisite solid solutions inclusive (epidote, actinolite, Fe–Mg chlorite, Ca–Mg–Fe carbonate). Solid solutions include the main ore (sphalerite, galena, chalcopyrite, bornite, chalcocite, pyrite, and pyrrhotite), ore-forming (quartz, muscovite, biotite, microcline, albite, and others), and metasomatic minerals (epidote, actinolite, chlorite, and others).

SIMULATION RESULTS

In considering the results, we focused much attention on Zn behavior, because the attainment of conditions of the ore formation is determined in compliance

with the following criteria: the formation of veins with bulk Zn contents equal to or exceeding 20 wt % (or sphalerite $\geq 30\%$) with layers of almost monomineral sphalerite in the cross sections of veins with Zn > 40 wt % (ZnS ~ 60–70%).

The chemical composition and properties of the ore-bearing hydrothermal solution are defined by conditions in the mobilization zone. This can be illustrated by the mobilization model at 370°C and 1000 bar (10 kg of granite, and f_1 as the average contents of ore components). The initial interaction between unaltered granite and primary solution (zero wave, 0W) produces equilibrium mineral assemblage corresponding to the weakly altered rock (quartz, microcline, albite, muscovite, epidote, chlorite, actinolite) with subordinate amounts of pyrrhotite, sphalerite, galena, and chalcocopyrite. Ore elements and sulfide sulfur enter the solution owing to sulfide dissolution with silicates as buffers.

The variations curve of Zn during sphalerite dissolution can be subdivided into four intervals by waves or “time”: (Fig. 2): (1) minimum solubility (1.6×10^{-4} m Zn) at high contents of S(II) (2.6×10^{-2} m) and pyrrhotite stability (early stages of water–rock interaction); (2) a drastic increase in solubility with decrease in S(II) (iron sulfides are absent, chalcocopyrite is replaced by bornite); (3) a plateau interval of extreme solubility of 1.9×10^{-3} m Zn (maximum solubility at given T and P); (4) the complete leaching of initial metal amount from the granite, so that the equilibrium solution becomes barren with respect to Zn. A similar situation but at lower contents and higher wave numbers (later “time”) is repeated for Pb and Cu.

Ore elements occur mainly as chloride complexes, with significant role of hydrosulfide complexes during the initial stages of galena dissolution. The Cu passage into solution is accompanied by a change in the main equilibrium mineral phase: chalcocopyrite during initial stages is subsequently replaced by bornite and chalcocite. This process occurs at a decrease in the total content of sulfide S owing to its leaching.

Figure 2 portrays the change of leading metal in the ore-bearing solutions during ore mobilization: Fe dominates during early stages under the highest S(II) content; if sulfide sulfur predominates over Fe, Zn becomes the main component, while Pb and Cu predominate at late waves. The acidity of the leaching solutions (pH 5.3), ionic strength (0.7), redox potential (Eh from -0.7 to -0.5 W), and the contents of other components (Na 0.9, K 0.2, Ca 0.006, Si 0.02, Fe 0.003, Mg and Al 0.0000n, Cl 1.1, C 0.5 m) remain practically constant during the passage of 30–40 waves of starting solution.

Each portion (wave) of the ore solution enters the fissured channel and begins ascending motions, which is divisible in the model into step reactors. The model vein body is formed in this channel owing to the gradual temperature decrease. Since portions (waves) of the solutions have different contents of ore elements and

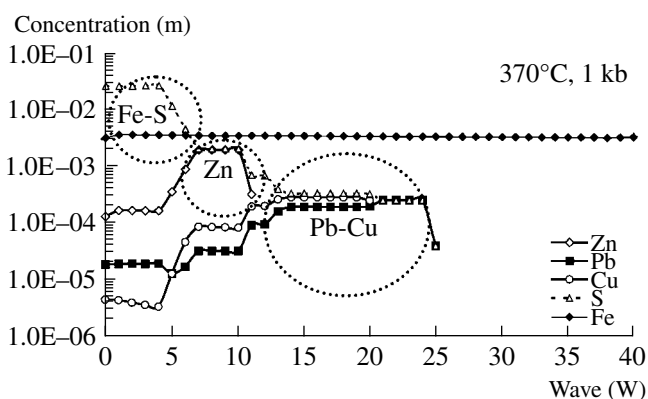


Fig. 2. Variations in the concentrations (mol/1000 g H₂O or m) of ore elements, sulfide sulfur, and iron in the leaching solution in the mobilization zone depending on the portion (wave) of the primary solution (370°C, 1000 bar, 10 kg granite with Zn content of 0.007% corresponding to f_1). Contoured fields are intervals (according to waves) of predominant metals.

sulfide sulfur, they precipitate different minerals when passing through the fissure.

Figure 3 illustrates some results of our simulation of ore formation (10 and 15 W) from the hydrothermal solution described above and in Fig. 2. Hereinafter, the left-hand figures show the bulk contents of minerals at different levels updip the simulated vein (from high to low temperatures); the right-hand plots show the internal structure of the vein at several levels updip the vein (from high to low temperatures).²

It is seen in the left-hand plots of Fig. 3 that the highest bulk sphalerite contents were approached at 130–150°C at 10–11 W, reaching 11.7–11.8 wt %. Its concentrations decrease with both increasing and decreasing temperature (below or above this level updip). The bulk ZnS content also shows a decrease at the earlier and later (by wave numbers) intervals of ore formation (for example, the transition from 10 to 15 W, Fig. 3). This is explained by the fact that Zn is completely leached from granite at 10–11 waves, at which it reaches the highest contents in the solutions at given T and P (Fig. 2). At different levels updip the simulated vein, its internal structure can be analyzed in the “layers” of minerals accumulated by the arrival of a certain wave. These data for updip levels corresponding to 150 and 200°C are shown in the right-hand plots in Fig. 3. It can be seen that the near-contact vein zone (layers 0–6) is composed of quartz and pyrite (from 0 to 50 wt %) at small contents of sphalerite (no more than 3.5%) and galena (no more than 1%). The abundant deposition of sphalerite begins only at wave 7 or at layer 7 and reaches a maximum of 27.9% at 140–150°C. In this local interval at 150°C, sphalerite precipitates only

² The figures do not show quartz, which often is the predominant mineral (20–100 wt %), and chlorite (accounting for up to 0.5 % only at high temperatures).

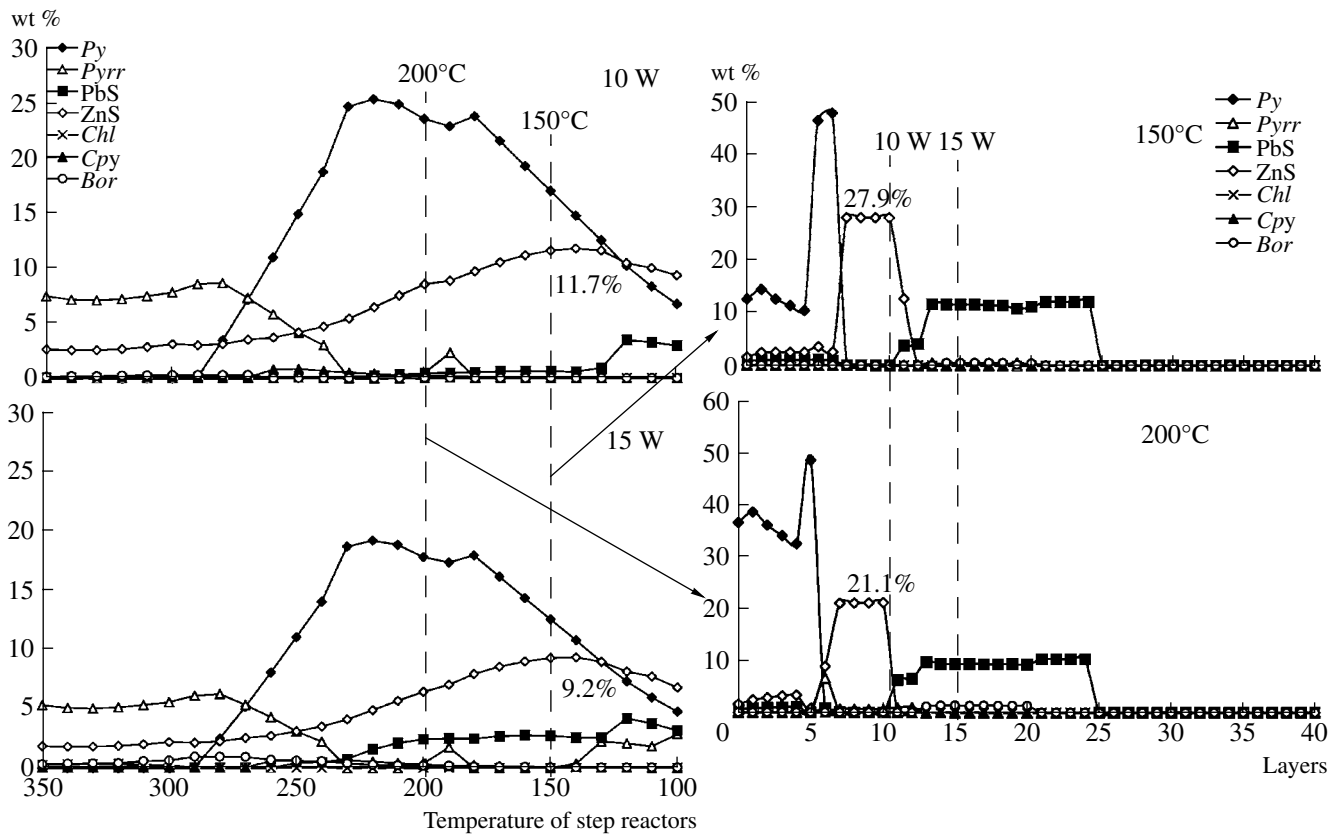


Fig. 3. Bulk contents of minerals at different levels up dip the model vein (left-hand plots) at 10 and 15 waves (W) and the internal structure of the vein at 150 and 200°C (right-hand plots) for the mobilization model at 370°C and 1000 bar (10 kg of granite with Zn content 0.007% corresponding to f_1). All minerals except quartz are present: (Py) pyrite, (Pyrr) pyrrhotite, (PbS) galena, (ZnS) sphalerite, (Cpy) chalcocopyrite, (Bor) Bornite, (Chl) chalcocite.

together with quartz (21.1%), and they are joined by trace amounts of chalcocopyrite (~0.7%) at 200°C. The bulk of galena begins to precipitate after ten waves (from layer 11). Most Cu minerals crystallized at higher temperatures (15W, Fig. 3). It is seen that four points at the plateau of extreme ZnS solubility in the mobilization zone (Fig. 2) are similar to those in the maximum of local crystallization of sphalerite in the cross-section of simulated vein (right side of Fig. 3). If the background Zn contents in the granites were taken to be two times lower (f_0), the vein simulated under the same conditions contains only 6 wt % ZnS and only one "layer" of concentrated sphalerite precipitation (27.9%) in the cross section of the vein.

The results show that changes in the system parameters are required to approach data observed in the Dzhimi vein. The intensity of sphalerite precipitation can be affected by external factors of ore formation: a temperature increase and/or a pressure decrease in the mobilization zone (as noted earlier [5, 14]). With a temperature increase and a pressure decrease, the solubility of sulfides increases, so that the same amount of metal will be leached from granite in the mobilization zone for a briefer time period and, respectively, precipitated in the vein within the lower number of "layers". An

increase in the bulk metal content in the system is affected by the internal parameter of ore-formation, the increase of background content of metal in the host rock (in the source of the ore components).

The effect of pressure at constant temperature was calculated for mobilization at 370°C and 600 bar (10–40 kg granite with an average Zn content of 0.007 or f_1), while the vein is formed at 350–100°C and 600 bar, i.e., all parameters except pressure and the range of rock/water ratio are analogous to those in the model considered in Figs. 2 and 3. Figure 4 illustrates the extraction of Zn from granite in the mobilization zone as compared to the results at 1000 bar. The pressure decrease results in an increase of sphalerite solubility. In particular, while the primary solution interacted with 30 kg of granite, the maximum Zn content was 0.0051 m at 16 W against 0.0019 m at 7–10 W and 1000 bar. The figures show that the amount of granite (rock/water ratio) also affected the attainment of the extreme solubility. At 10 and 20 kg, the calculation step in rock/water ratio is too large to record the maximum solubility of ZnS, though the Zn content begins to increase from its minimum level (about 0.0009 m). The extreme (maximum) solubility is steadily attained by interaction with 30–40 kg of granite and more. With increasing

rock/water ratio, the plateau of the extreme solubility is shifted toward greater numbers of waves and, hence, the process is prolonged in time.

The simulation results for vein forming from these solutions are shown in Fig. 5 (mobilization zone at 370°C, 600 bar, 30 kg granite with an average Zn content of 0.007% or f_1). The maximum bulk content of sphalerite in the vein is 20.3% at 16–17W, while almost monomineral “layers” (ZnS up to 58.7%) in the cross section of the simulated vein are formed at 130–140°C. For convenient comparison of diverse models of ore formation, results in this and subsequent figures will be shown for fixed time intervals (15 and 20 W, right-hand plots) and temperature updip the vein (150 and 200°C, left-hand plots).

As can be seen from Figs. 3 and 5 (1000 bar and 10 kg against 600 bar and 30 kg under other equal conditions), an increase in the rock/water ratio in the mobilization zone shifts the maximums of sphalerite precipitation in wave numbers (bulk) and layers (localization in cross sections). The pressure decrease causes a more than two-fold increase in pyrite precipitation, as is seen from the plots of the bulk contents and vein cross-sections. Up to 20% pyrite is precipitated at wave 15 at 1000 bar, and more than 55% is precipitated at 600 bar. A similar situation is observed for pyrite in the near-contact zone: 10–50% at 150°C and 35–50% at 200°C and 1000 bar, 45–60% and 60–65% at 600 bar (right-hand plots in Figs. 3 and 5). Greater amounts of sphalerite and galena (up to 13–16% ZnS and ~3–4% PbS at 150°C against 3.5 and 1%, respectively, at 1000 bar) crystallize simultaneously with pyrite in this zone at 600 bar. This fact is illustrated in Fig. 4, in which the minimum solubilities of sphalerite in the mobilization zone under these conditions differ by one order of magnitude, while these solutions are responsible for the precipitation of ore minerals in the near-contact zones of the simulated vein. The solubility of pyrrhotite, galena, and chalcopyrite also significantly increases in the mobilization zone at 600 bar. It should be noted that late (relative to pyrite and sphalerite) pyrrhotite appears at 600 bar. Pyrrhotite occurs in 18–20 layers at 150°C immediately after the maximum of sphalerite precipitation. This mineral seemingly separates sphalerite and galena intervals in the vein cross-section. However, if the orebody had been formed by wave 17 or the given cross section of the vein corresponds to a temperature of 170–220°C, no pyrrhotite crystallized (for example, 200°C at the right-hand plot of Fig. 5). At temperatures higher than 230°C, pyrrhotite precipitated in the first “layers,” i.e., prior to pyrite crystallization.

Thus, a bulk sphalerite content of 20.3% (16–17W, 130–140°C) and a maximum content of up to 58.7% in 15–16 layers of the vein cross section were attained in the mobilization zone (at f_1) by simulating ore formation at 600 bar and 370°C. The first numeral is three times lower than that found in the natural veins, but the

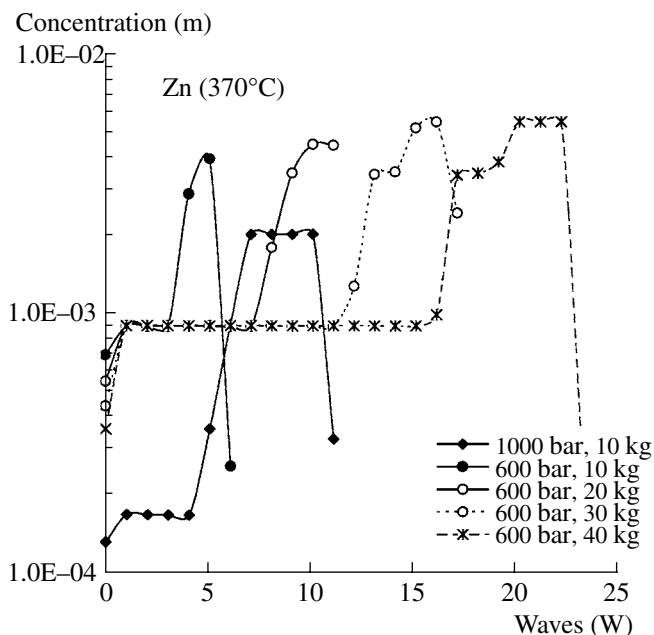


Fig. 4. Variations in the Zn content in the leaching solution in the mobilization zone depending on the portion (wave) of the primary solution at 370°C, 600 and 1000 bars, and various rock masses (f_1).

second numeral is already close to them. Close values of 20.9% (15W) and 59.3% (14–15 layers) were obtained in the mobilization zone for the model at 700 bar and 380°C.

The effect of temperature at a constant pressure was estimated in a series of calculations for mobilization at 400, 410, and 420°C and 1000 bar (10–100 kg of granite with a Zn content corresponding to f_1), while vein is formed from 380–400°C to 100°C and 1000 bar, i.e., all factors are the same as in the models considered in Figs. 2–3, except the temperature and a larger number of reactors in the vein. Figure 6 portrays the results on sphalerite solubility in the mobilization zone at 370–410°C (all at 1000 bar). The temperature increase results in a significant increase of the Zn content. The extreme solubility at different temperatures is reliably determined at different masses of starting granite: 0.0019 m (10 kg) at 370°C, 0.0051 m (20 kg) at 400°C, and 0.0069 m (30 kg) at 410°C. At 420°C, the extreme solubility was found only at 100 kg (one point of 0.0095 m at 35 W). Even the minimum solubility at 420°C (~0.0021 m Zn) exceeds the extreme solubility at 370°C.

The ore formation plots presented in Figs. 7 and 8 are very similar. At a starting temperature of 400°C, the maximum bulk ZnS content is 22.6% (15 W, 140°C) and the local content is 53.1% for 12–15 layers in the vein cross section at 140°C (Fig. 7). At 410°C, the bulk ZnS content is as high as 23.5% (12 W, 140°C) and that in the vein cross section is 61% in 11–12 layers at 140–150°C (Fig. 8). An increase in the solubility and

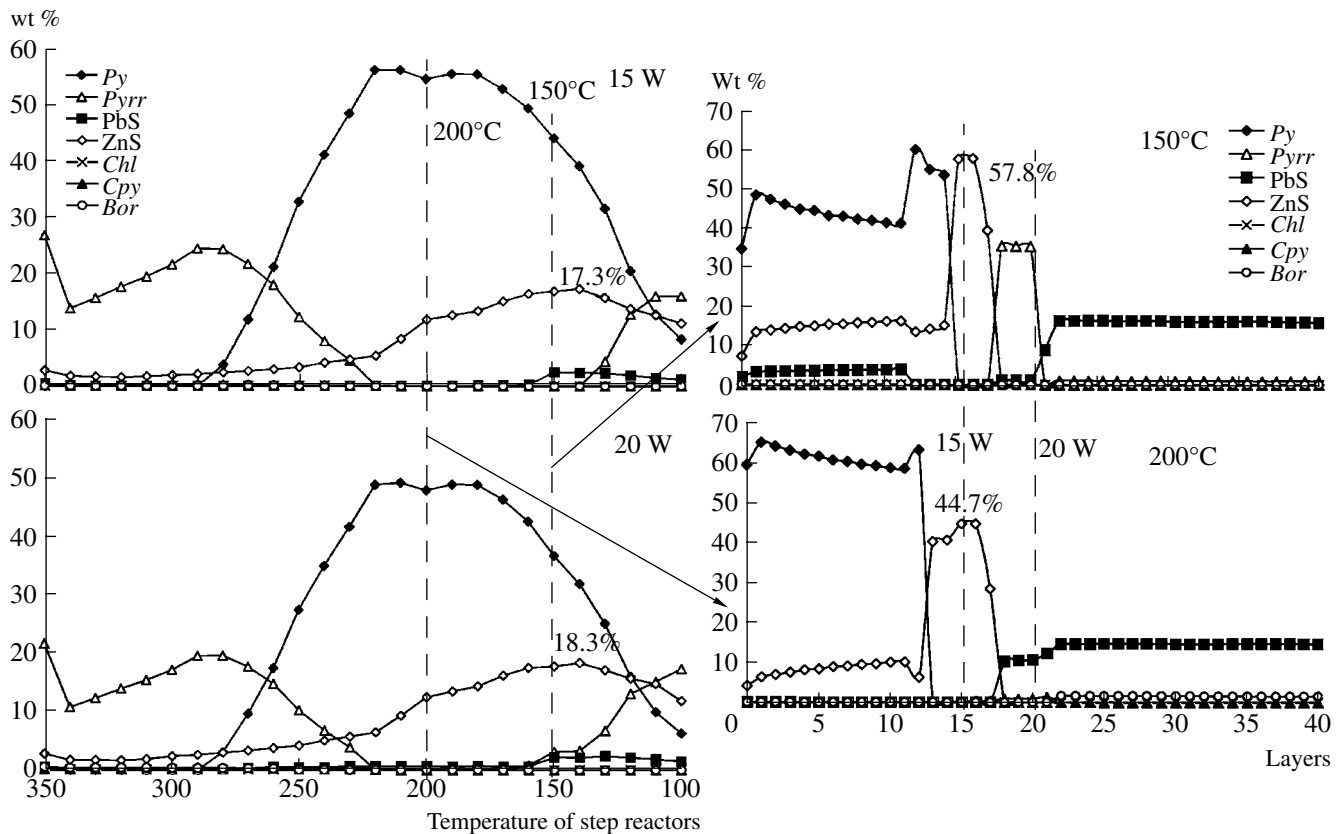


Fig. 5. Bulk contents of minerals at various levels up the model vein (left-hand plots) at 15 and 20 waves (W) and the internal structure of the vein at 150 and 200°C (right-hand plots) for the mobilization model at 370°C and 600 bar (30 kg granite with Zn content 0.007% corresponding to f_1).

temperature brings about a change in the mineral proportions in the near-contact zone of the vein. In particular, the vein level of 150°C contains from 21 to 30% pyrite (one maximum of up to 60% in layer 11), 10–12% sphalerite, and 3–3.6% galena at a starting temperature of 400°C (Fig. 7); these values are, respectively, 25–32%, 15–18%, and 4.4–5% at a mobilization temperature of 410°C (Fig. 8). Significantly higher pyrite contents (up to 50–60%) were recorded at deeper levels (at 200°C). At this temperature, the near-contact zone shows a decrease in sphalerite and the almost complete absence of galena. As in the above models, no late pyrrhotite is formed at 200°C.

At starting conditions of 420°C and 100 bar (up to 30 kg of granite with f_1), the step of division of the flowing system was so large that no extreme solubility of sphalerite was attained (only its growth was noted). Therefore, the formation of practically monomineral sphalerite layers in the vein cross section is skipped in the theoretical models of ore formation. This is a disadvantage of the simulation technique. The local sphalerite maximum (very narrow) was also presumably formed under these conditions but could be calculated only at a higher primary rock/water ratio in the mobilization zone (100 and more). It is possible that the point

at 420°C and 1000 bar (at f_1) separates different conditions of ore formation. The near-contact zone of the vein simulated at these starting conditions exhibits very high contents of sphalerite (up to 23.6%) in association with quartz, pyrite, and galena (up to 6.6%), which is quite evident for such a high minimum (0.0021 m Zn) solubility of sphalerite.

Thus, it was shown that, in the series of 370, 400, 410, and 420°C (at 1000 bar), Zn content in the ore-bearing solution shows a systematic increase, while the leaching time of the initial zinc content decreases. This causes an increase in the bulk content of sphalerite, its precipitation level in the near-contact zone, and local maximums in the vein cross section. However, if an extreme solubility similar to that at 420°C is not attained, the monomineral “layer” with a local maximum of sphalerite precipitation is not formed in the vein cross-section.

To exemplify the ore formation with no monomineral sphalerite layer, let us consider the internal structure of the vein formed under the initial conditions in the mobilization zone of 400°C and 600 bar (30 kg, f_1) (Fig. 9). Under these conditions, the Zn content in the ore-bearing solution is 0.0077 m, which is significantly higher than that in most of the previously considered

situations. However, this is only the minimum (!) solubility of sphalerite, while its extreme solubility is not even approached at all. As is seen in Fig. 9, the near-contact zone of the vein (layers 0–5) contains a significant amount of sphalerite (up to 37%) in association with 53–60% pyrite (later, up to 85%), with no monomineral sphalerite “layers”, which were found in all of the aforementioned models immediately after the deposition of the early quartz–pyrite–sphalerite–galena mineral assemblages. It should be noted that the intensification of pyrite precipitation in the near-contact zone is typically observed at low pressures (simulation results for vein cross sections at 150°C at initial conditions of 1000 and 600 bars and 370°C in Fig. 3 and 5 or 400°C in Figs. 7 and 9).

Now we can generalize the preliminary results. In the models considered above (at Zn content in the granite corresponding to f_1), the highest bulk Zn contents of 20.3–23.5% were obtained at starting conditions of 400–410°C and 1000 bar, Zn contents of 20.3–20.9% were formed at 370–380°C and 600–700 bar. The maximum local contents of sphalerite in the individual layers reached 53–61% in the formed case and 58.7–59.3% in the latter.

These models are characterized by the following common features in the mobilization zone:

1. These conditions make it possible to reliably reach the limiting (maximum) solubility of sphalerite from granite. If this is not the case (the sphalerite solubility is at a minimum at given T and P), no monomineral sphalerite layer is formed in the cross section of the vein. An increase in the rock/water ratio (up to 100 in our calculations) does not modify the final result.

2. At a Zn content in the ore-bearing solution of $\sim 5 \times 10^{-3}$ m (370°C and 600 bar, 400°C and 1000 bar), the bulk sphalerite content is no more than 20.3–22.6% and the local sphalerite content in the monomineral layers is up to 53–58.7%.

3. If the extreme solubility reaches values close to 7×10^{-3} m, the sphalerite content shows a further growth (up to 23.5% for the bulk content and 61% for the practically monomineral “layers”). This result was obtained in the ore formation model at starting conditions in the mobilization zone of 410°C, 100 bar (30 kg of granite with a Zn content corresponding to the average content or f_1).

Thus, the attainment of extreme (limiting) solubility of sphalerite in the mobilization zone and its further growth above 7×10^{-3} m Zn are required to reach the bulk sphalerite contents of 30% and local contents of 60–70% in the almost monomineral “layers” in cross sections. If the solubility is lower than 7×10^{-3} m (the plateau of limiting solubility is reached), veins are formed with bulk contents of less than 23% and layers with no more than 60–61% sphalerite. If a plateau of the limiting solubility is not attained, no monomineral layers are formed in quartz–pyrite–sphalerite veins at any Zn content in the ore-bearing solution (the level of

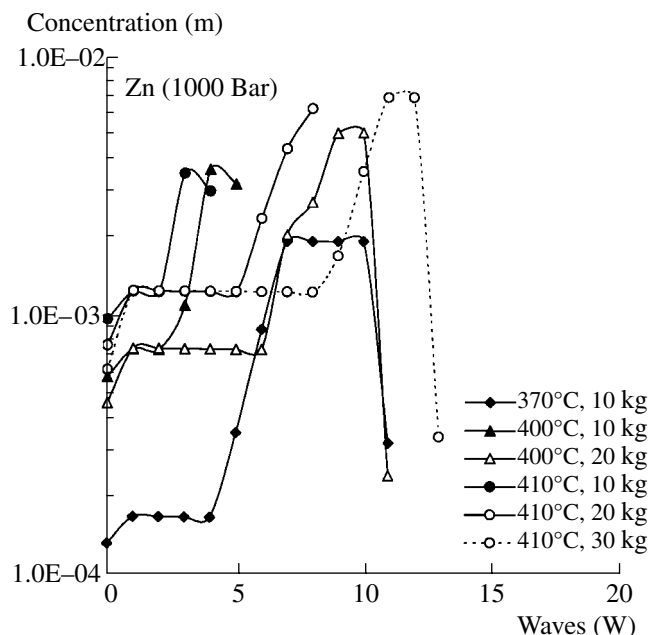


Fig. 6. Variations in the Zn content in the leaching solution in the mobilization zone depending on portion (wave) of the primary solution at 1000 bar, 370–410°C, and various rock masses (f_1).

the minimum solubility at given T and P could be high enough).

To determine the initial conditions providing the required result, we constructed a T - P diagram (Fig. 10). This diagram demonstrates all calculated points in the mobilization zone; Zn isoconcentrates at the level of extreme (maximum) solubility of sphalerite at given T and P ; lines of rock/water ratio for various background Zn contents in the granite (starting rock/water ratio = 100), which frame the T - P field of the attainment of the extreme sphalerite solubility (extreme Zn contents are attained below this line and are not achieved above it).

It can be seen that an increase in the background Zn content in granite (from f_0 to f_2) expands the P - T field of the mobilization zone toward higher temperatures and lower pressures, at which the extreme (maximum) sphalerite solubility can be achieved. In addition, the diagram demonstrates starting points for the ore formation models. In most of the previous models, the calculations were conducted for a background Zn content corresponding to 0.007% or f_1 . The upper (f_1) and lower (isoconcentrate of Zn of 7×10^{-3} m) constraints determine a very narrow T - P range of the maximum sphalerite precipitation. Only one of the ore formation models plots in this T - P range: 410°C and 1000 bar (30 kg granite with f_1). However, these starting conditions provided only 23.6% of the bulk sphalerite content (or about 16% in recalculation to Zn) and 61% in individual “layers” across the vein, which are insufficient.

It is interesting to identify the parameters that could cause the growth of the bulk sphalerite content in the

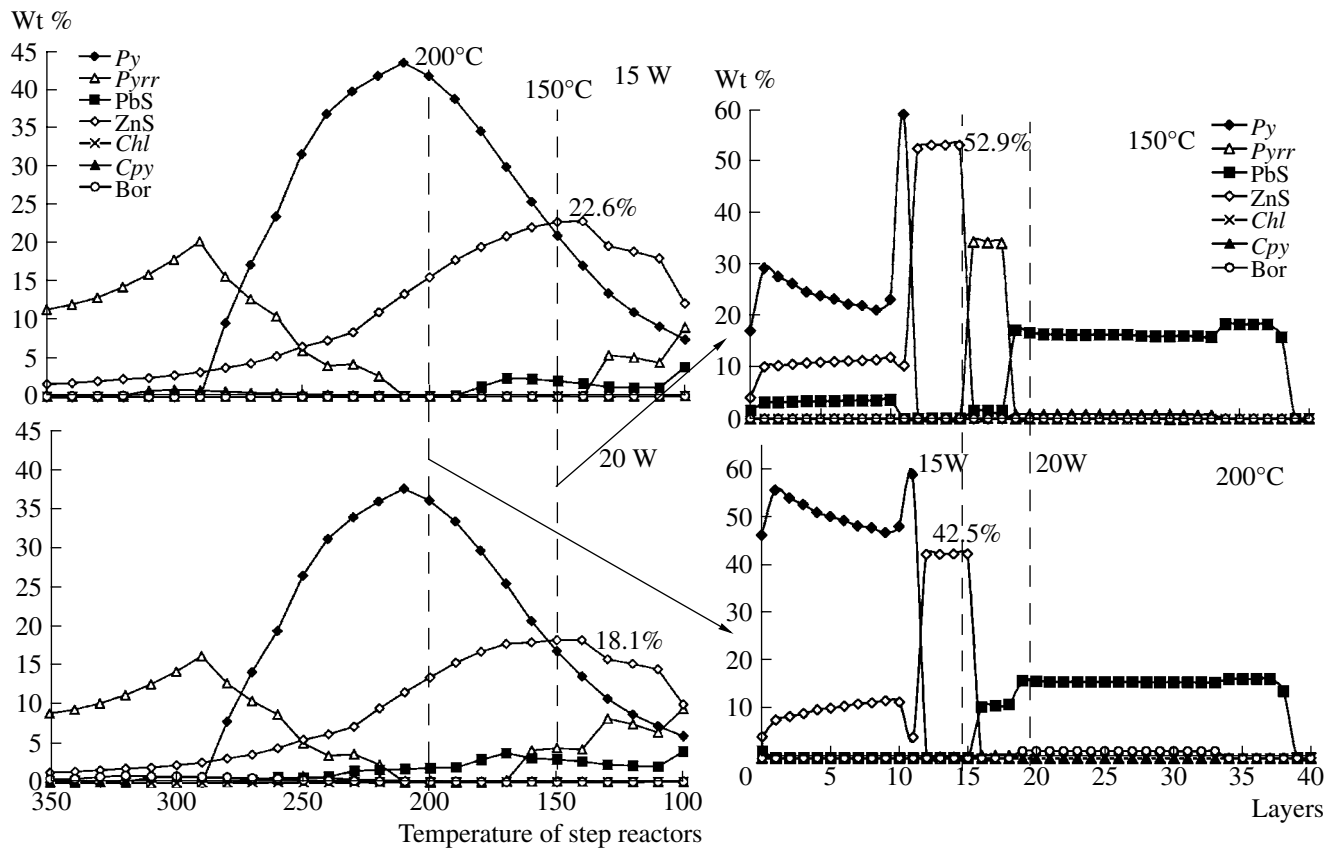


Fig. 7. Bulk contents of minerals at discrete levels up dip the model vein (left-hand plots) at 10 and 15 waves (W) and the internal structure of the vein at 150 and 200°C (right-hand plots) for the mobilization model at 400°C and 1000 bar (30 kg of granite with Zn content 0.007% corresponding to f_1).

veins. The temperature and pressure exert no required effect (at background Zn content corresponding to f_1), as is shown in Fig. 10, because a shift to temperatures higher than 440°C (which requires a simultaneous growth in pressure is hardly possible in light of data on fluid inclusions). The mobilization zone can be widened in T and P if the granites have elevated background Zn contents (for example, up to 0.01 wt % or f_2). In Fig. 10, the gray field outlines the T - P conditions of mobilization under which veins can be formed with the maximum concentrations sphalerite contents and its almost monomineral layers of sphalerite in the cross-sections. This field has an upper limit corresponding to the rock/water line at f_2 and a lower limit at the isoconcentrate of the extreme sphalerite solubility of 9×10^{-3} m Zn. Let us examine the effect of background Zn content on the efficiency of ore formation.

Figure 11 shows the results of our simulations of the ore formation at starting conditions of 410°C and 1000 bar (30 kg of granite with elevated background Zn contents or f_2), i.e., all parameters other than background Zn content in granite are analogous to those in the aforementioned model (Fig. 8). The extreme (maximum) sphalerite solubility in the mobilization zone remains

the same (0.0069 m); however, four instead of two points plot in the concentration plateau. The maximum bulk content of sphalerite increases from 23.6 to 28.8% (14W). High bulk contents of 27.6 and 22.9% are also observed later at waves 15 and 20, respectively. However, the Zn contents in the monomineral sphalerite remain at the same level of 61%, because the solubility of sphalerite in the mobilization zone remains unchanged. This local maximum spans more "layers," from 11 to 14, i.e., four points plot on the plateau of the maximum solubility of sphalerite in the mobilization zone. This widening provides an increase in the bulk sphalerite content in the vein.

The simulation results of ore formation at starting conditions in the mobilization zone at 430°C and 1100 bar (30 kg of granite with elevated background Zn content or f_2) are shown in Fig. 12. The point of the assumed conditions is located in the center of field favorable for ore formation in Fig. 10. Under such parameters, sphalerite reaches its extreme solubility, the two points at 1×10^{-2} m Zn. In contrast to the previous models, new results are presented in detail: 10, 15, 20W and cross-section at 160 and 200°C, because the maximum sphalerite contents were reached at 10W and 160°C. It is seen that a bulk sphalerite content of 31.3% occurred

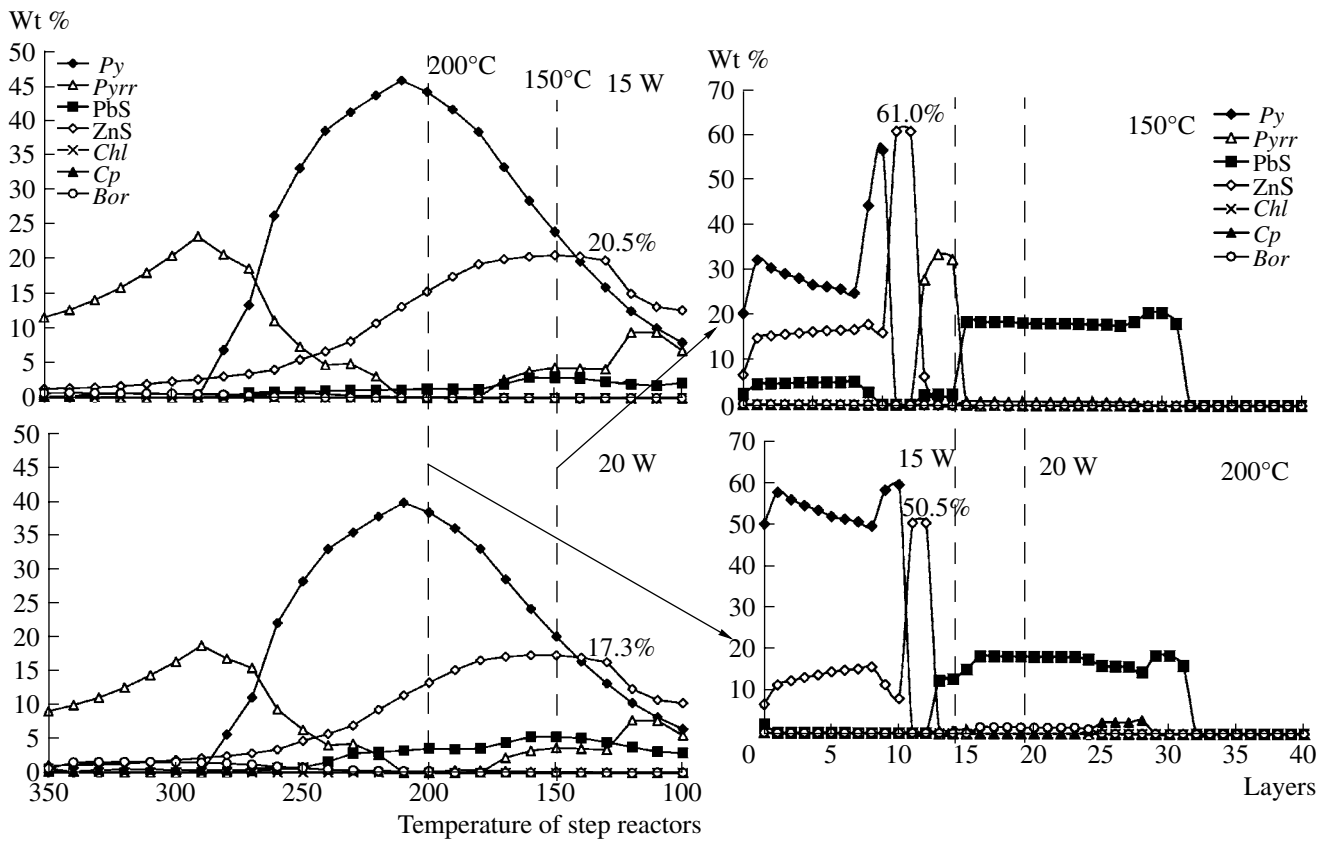


Fig. 8. Bulk contents of minerals at discrete levels updip the model vein (left-hand plots) at 15 and 20 waves (W) and the internal structure of the vein at 150 and 200°C (right-hand plots) for the mobilization model at 410°C and 1000 bar (30 kg of granite with Zn content 0.007% corresponding to f_1).

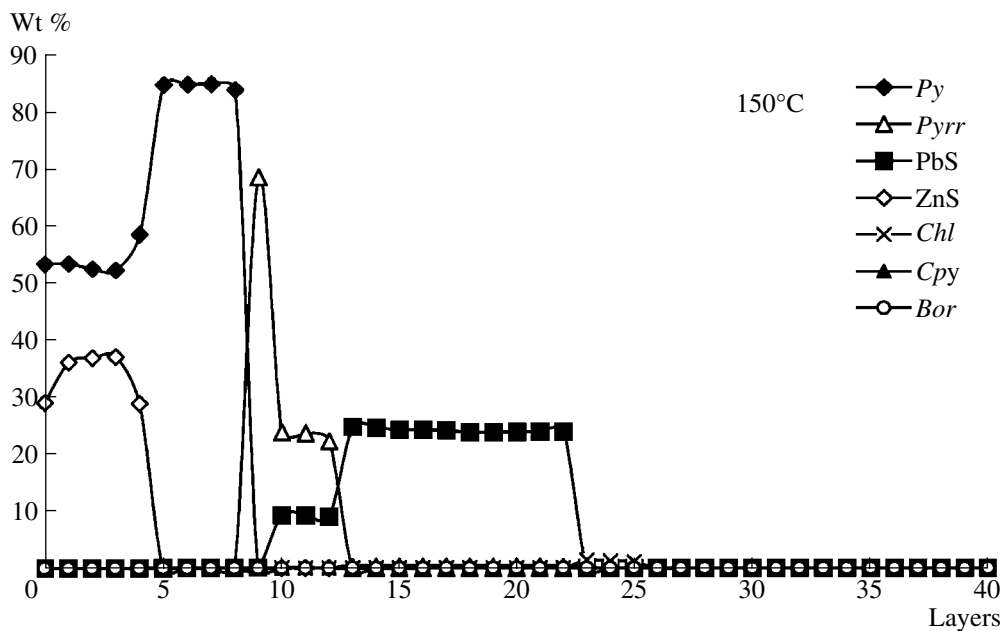


Fig. 9. Distribution of minerals across the vein at a level of 150°C for the model with starting conditions of 400°C and 600 bar (30 kg of granite with Zn content of 0.007% corresponding to f_1).

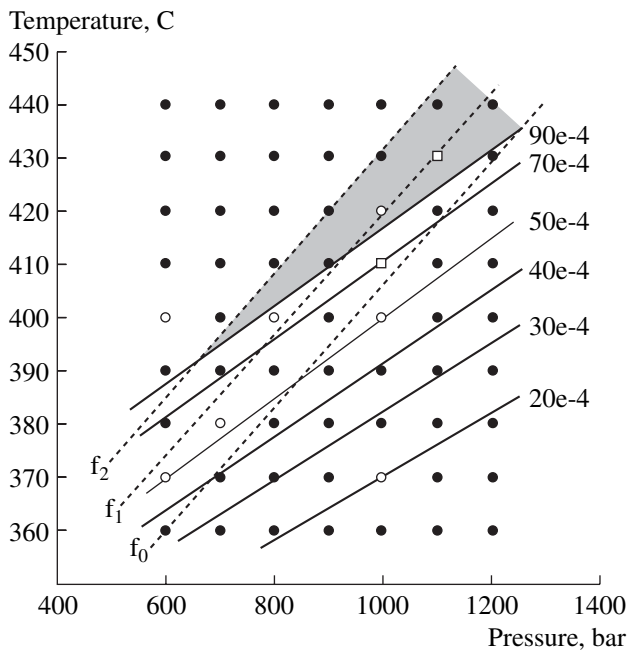


Fig. 10. T - P field in the mobilization zone (shaded area) most favorable for the production of ore-bearing solutions that form rich Zn ores with the maximum (~30% and more) bulk contents of sphalerite and local contents in vein cross-section (60–70% and more). Symbols: solid lines are is-concentrates of The extreme (maximum) solubility of sphalerite (Zn, mol/1000 g H_2O); solid circles are calculation for the mobilization zone; open circles are calculations from the mobilization zone to ore formation in the vein (at average Zn content in the granite of 0.007% corresponding to f_1); open boxes are calculations from the mobilization zone to ore formation in the vein (at elevated Zn content in the granite of 0.010% corresponding to f_2); the dashed line denotes the limiting rock/water ratios at various Zn contents in the starting granite (f_0 , f_1 , f_2) constraining T - P region from top, where extreme (maximum) sphalerite solubility is attained.

at wave 10 at 160°C, in association with 28.8 and 3.4% of pyrite and galena, respectively. The interval of practically monomineral sphalerite precipitation (67.4% in waves 9 and 10) in association with quartz was obtained at 160°C. The near-contact part of the vein (waves 0–8) at 160°C has the following mineral proportions: 30–37% pyrite (up to 52%), 21–26% sphalerite, ~6% galena, and quartz. The bulk of galena is deposited after “late” pyrrhotite (21–24% in layers 14–25). Up to 1% chalcopyrite precipitates along with galena. At 200°C, the precipitation succession and the proportions of minerals in the cross section change: the near-contact part contains pyrite (about 50%) and sphalerite (up to 21.5%) without galena, which is followed by a zone of practically monomineral sphalerite in layers 9–10 (59.1%), and late galena and chalcopyrite (~3%) without pyrrhotite. Later (at 15 and 20W), the bulk contents of sphalerite and pyrite decrease, while that of galena increases and is coupled with the widening of the field of its crystallization temperature.

Thus, the temperatures of 410–440°C, pressure of 900–1200 bar, and host granites with elevated background Zn contents (more than 0.007 wt %) are required to simulate an ore vein in which the bulk sphalerite content reaches or exceeds 30%, and an almost monomineral sphalerite “layer” (ZnS at 60–70%) is formed in the cross section.

DISCUSSION AND COMPARISON WITH FACTUAL DATA

When formulating the problem, we have focused much attention on the attainment of the maximum sphalerite contents (bulk contents and local contents in the almost monomineral “layers”). However, our results can provide much more information, because they describe the tendencies in the distribution of all minerals composing the vein: quartz, pyrite, pyrrhotite, sphalerite, galena, chalcopyrite and others. Therefore, we decided to compare the distribution of Fe, Zn, Pb, and Cu in natural and modeled veins. In comparing them, we used models in which sphalerite contents most resemble those observed in natural veins.

The Tsentral'naya vein has the following bulk contents of metals: Fe 17.1, Zn 18.7, Pb 4.2, and Cu 0.15 wt % (table). In recalculation for the main minerals, the vein contains 36.4 FeS_2 , 27.9 ZnS, 4.8 PS, and 0.6 wt % $CuFeS_2$. Using this scale, we attempted to select time intervals and levels up the vein at which certain model veins were formed. For the model with starting conditions of 430°C and 1100 bar in the mobilization zone (left-hand side of Fig.12), the boundaries are clearly distinguished by temperature and waves: from 180 to 200°C (temperature level up the vein) and from 17 to 20 W (“time” interval of the evolution of hydrothermal system). Within these boundary conditions, the following bulk mineral composition of the model vein was obtained: FeS_2 27.6–36.6, ZnS 18.4–23.7, PbS 3.1–5.0, and $CuFeS_2$ 0.3–0.7 wt %. These values are in a good agreement with the actual contents of pyrite, galena, and chalcopyrite in the bulk sample along the cross section of the Tsentral'naya vein. The simulated contents of sphalerite under these boundary conditions were somewhat lower; however, some increase in the background Zn content in granites or in temperature (within T P field favorable for mobilization) will lead to the complete compatibility. In this model, the ZnS content corresponding to those in the natural vein are also achieved, but at the earlier “time” intervals (for example, up to 29% at 180°C and 10–11W or up to 28–31% at 160°C and 10–12W). This improves the consistency with the factual data on pyrite (up to 39–45% at 180–200°C and 10W), but, on the other hand, sharply decreases the consistency on galena and chalcopyrite, whose contents significantly decline (less than 1% PbS and 0.1% $CuFeS_2$). Lower temperatures (up to 160°C) are favorable for the growth of sphalerite and galena contents (Fig. 12), but bring about

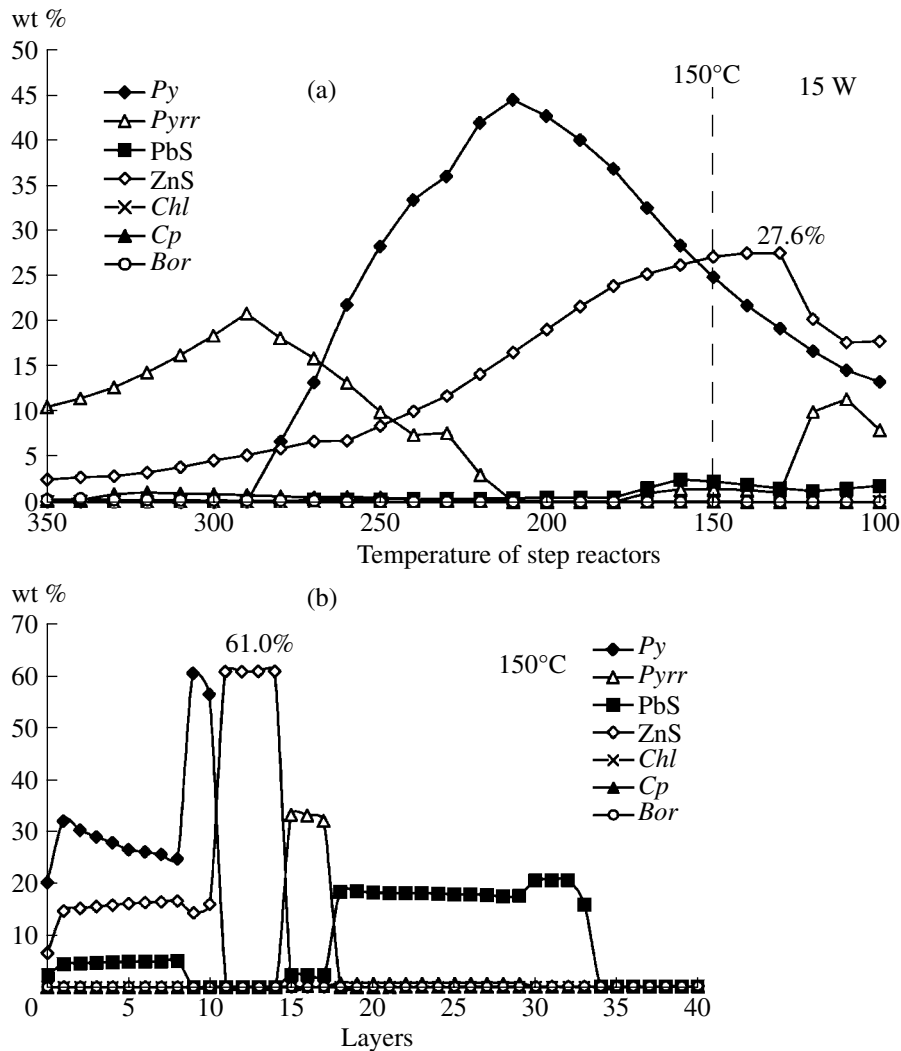


Fig. 11. Bulk contents of minerals at various levels up dip the model vein (a) at 15 wave (W) and the internal structure of the vein at 150°C (b) for the mobilization model at 410°C and 1000 bar (30 kg granite with Zn content of 0.010% corresponding to f_2).

decrease in pyrite content up to its prevalence, which is not observed in the natural vein. At temperatures above 200°C, the contents of sphalerite and galena begin to significantly decrease. This allowed us to constrain the ranges of temperature and waves for the subsequent analysis (simulations were conducted for 40 solution waves, which form vein body in 33 reactors with temperatures from 410 to 100°C), i.e., determine the level in depth and “time,” which corresponds to the studied section across the Tsentral'naya vein.

Let us compare the simulation results for the same model but within limited conditions of 180–200°C and 17–20W with data on the mineral distribution across the natural veins. Figure 13 illustrates data on Fe, Zn, Pb, and Cu distribution in the cross-section of the Tsentral'naya vein, Bozang ore zone (sampling of the year 2003, sampling step 4 cm, inset 26, Severnyi drift, adit 47, Dzhimi deposit). The Zn distribution exhibits two maximums in the central parts of the vein (28.8% at an

interval of 16–20 cm and 25.7% at 36–40 cm) and an absolute maximum in the near-contact part (40% at 52–56 cm). High Fe contents were found in the near-contact part (up to 20.6% at 0–12 cm) and in the central parts of the vein (20.5–21.9% at 24–32 cm and 20.3–21.1% at 40–48 cm). The absolute Fe minimum (9.5–9.8%) coincides with the maximum Zn content. The highest Pb content coincides with one of the Zn maximums (10.3% Pb at 16–20 cm). A main Cu maximum was found at 36–40 cm (up to 0.6%).

Some of the simulation results that can be compared with natural data are shown in the right-hand plots of Fig. 12, which demonstrate the distribution of minerals in the layers of the model vein from contact (layer 0) to the center (layers 20–40). As is seen in Fig. 12, the distribution of minerals in the cross-section of the model vein reveals a distinct stratified character: (1) a near-contact zone is composed of the early quartz–pyrite–sphalerite–galena assemblage, which is dominated by

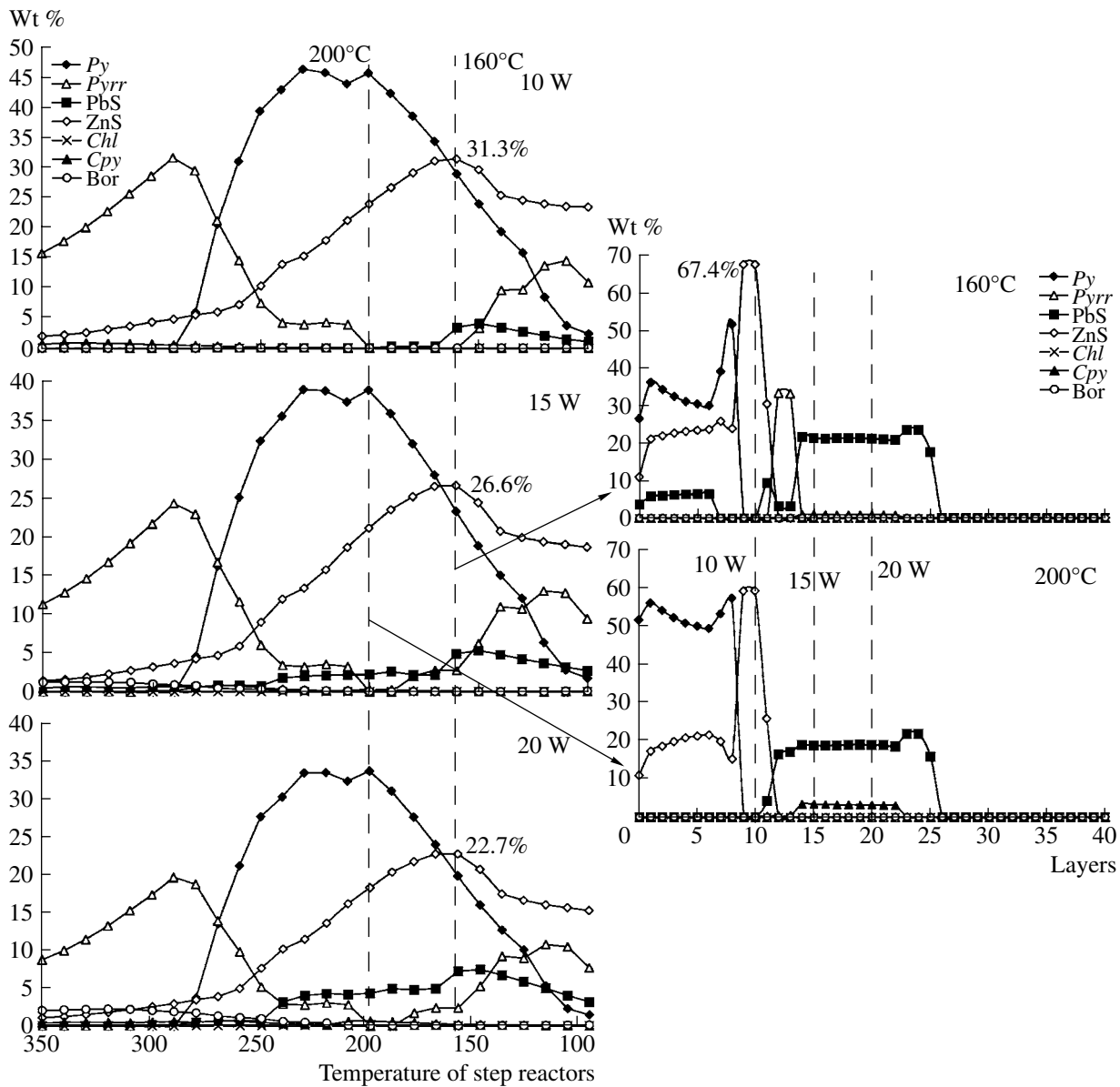


Fig. 12. Bulk contents of minerals at various levels up the model vein (left-hand plots) at 10, 15, and 20 waves (W) and the internal structure of the vein at 160 and 200°C (right-hand plot) for the mobilization model at 430°C and 1100 bar (30 kg granite with Zn content of 0.010% corresponding to f_2).

pyrite (35–60% depending on the temperature level) at high contents of sphalerite (up to 20%) and significantly lower contents of galena (0–6%) and chalcopyrite (up to 0.03%);³ (2) a zone of practically monomineral sphalerite (up to 60–70%) with quartz and trace amounts of galena and chalcopyrite (up to 0.3%) with no pyrite (this zone is shifted from the contact and formed later); (3) the main precipitation zone of the quartz–galena–chalcopyrite assemblage dominated by quartz, with up to 15–21% galena and up to 3.5% chalcopyrite (at temperatures < 160°C, the interval of pyr-

³ Quartz adds to 100%.

rotite precipitation can arise between zones 2 and 3); (4) the quartz core of the vein (25–40W).

The natural vein (Fig. 13) shows no such distinct differentiation of minerals. This fact can be explained as follows: The Tsentral'naya vein is at the sampling site (thickness of 60 cm and more) a massive sulfide body with a small amount of visible quartz. The vein morphology and microscopic data distinctly demonstrate that the vein formed in several time intervals. The earliest massive quartz–pyrite–sphalerite body was later broken by fissures into a number of permeable zones. During the second stage, these zones were penetrated by solutions that precipitated mainly sphalerite.

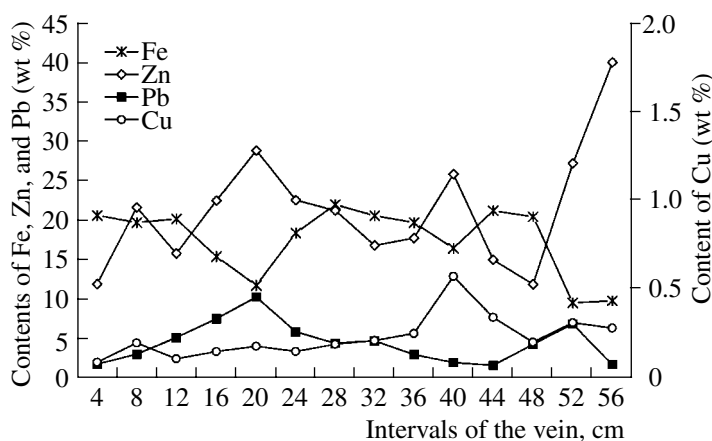


Fig. 13. Distribution of Fe, Zn, Pb, and Cu along the cross section of the Tsentral'naya vein (sampling step of 4 cm).

The amount of the precipitated sphalerite is determined by the free space in a given permeable zone. At the third interval, the "leading" mineral is replaced by galena and chalcopyrite.⁴ Galena and chalcopyrite could crystallize both in the early permeable and newly formed zones. Thus, the vein formation was accompanied by the superposition of mineral assemblages of different stages. This explains the several Zn maximums and the coincidence of Zn and Pb maximums in a single interval.⁵

Such a complex evolution of the vein complicates its direct comparison with simulated data and requires the selection of sampling intervals dominated by mineral assemblage that correspond to definite time interval of ore formation.

According to the simulations, the first time interval is characterized by a high Fe content and relatively low Zn, Pb, and Cu contents. These conditions are satisfied by the first sampling interval (0–4 cm), which contains 20.6 Fe, 12 Zn, 1.8 Pb, and 0.09 wt % Cu or, in recalculation, 43.8 FeS₂, 17.9 ZnS, 2.1 PbS, and 0.26 wt % CuFeS₂.⁶ The model of ore formation (right-hand part of Fig. 12) simulated 39.5–57.1 FeS₂, 11–25.3 ZnS, 0–3.9 PbS, and 0.02–0.03 wt % CuFeS₂ in layers 0–8 at 180–200°C. The values obtained for pyrite, sphalerite, and galena in natural vein correspond to those in the model vein. The content of chalcopyrite in the model vein was 8–10 times lower. This disagreement is related to the superposition of later material on the earlier mineral assemblage, which leads to a 0.3–3% increase in

the chalcopyrite content, as was demonstrated above, when the mineral differentiation in the model vein was described.⁷ In natural veins, minerals typically precipitated not parallel to the conduit contact or cutting lines that separate samples. Therefore, narrow "bands (layers)" of sphalerite and galena with chalcopyrite can occur in different samples. This is confirmed by data on the sampling interval of 28–32 cm, in which the content of pyrite (43.6%) and sphalerite (25%) are in good agreement with model boundaries, while those of galena and chalcopyrite are significantly higher: 5.4 and 0.6%, respectively. This suggests that the sample contains material of the later quartz–galena–chalcopyrite assemblage.

The quartz–sphalerite or the second time interval can be best characterized by sampling data on the interval at 52–56 cm with the highest Zn contents (Fig. 13), which, in recalculation to minerals, contains: 20.7 FeS₂, 59.7 ZnS, 1.9 PbS, and 0.08 wt % CuFeS₂. In the same model at 180–200°C (Fig. 12), layers 8–11 contain 0–57.1 FeS₂ (maximum only in layer 8), 15.2–64.5% ZnS (59–64.5% in layers 9–10, with minimums in layers 8 and 11), 0–7 PbS (4–7% only in layer 11), and 0.1–0.3 wt % CuFeS₂. Thus, there is a good agreement between the model and natural data on pyrite, sphalerite, and galena. The chalcopyrite content can be increased by assuming that this sample contains the material of the galena assemblage (a nearby sample contains a local galena maximum of up to 7 wt % and a higher Cu content).

The quartz–galena assemblage with chalcopyrite is most distinctly expressed only in one sample at the interval of 16–20 cm, but this sample shows a local Zn maximum (up to 28.8%). Recalculation to minerals yields the following composition: 25 FeS₂, 42.9 ZnS, 11.8 PbS, and 0.5 wt % CuFeS₂. In layers 12–20 of the

⁴ There is a positive correlation with data on the mobilization zone, which was described above and shown in Fig. 2.

⁵ It is clearly seen in polished samples of the vein and polished sections across it that the bulk of galena was precipitated later than and separately from sphalerite. The high Zn contents and the maximum Pb content in a single sample (an interval of 16–20 cm) is predetermined by the sampling step.

⁶ The calculations did not take into account that Fe is partially incorporated in chalcopyrite and in the ZnS–FeS solid solution (up to 5% Fe of total Zn content according to our data).

⁷ The Cu content can also be increased in the model by allowing for the sphalerite–chalcopyrite solid solution.

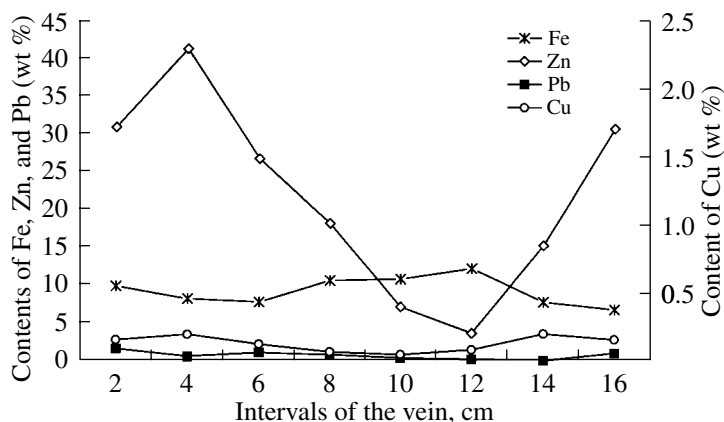


Fig. 14. Distribution of Fe, Zn, Pb, and Cu along the cross section of the Zapadnaya-3 apophysis (sampling site of 2 cm).

model, no pyrite or sphalerite are formed, while the PbS content varies from 15 to 21.8% and CuFeS_2 varies from 0.3 to 3.4 wt %. Evidently, three time intervals of ore formation were overlapped in this cross-section, which caused the “dilution” of the high contents of galena and chalcopyrite and the appearance of significant amounts of pyrite and sphalerite.

The second time interval (sphalerite) can be described by data on apophyses. Figure 14 demonstrates data on the distribution of main metals in the cross-section of the Zapadnaya-3 apophysis of the Bozang ore zone (year 2003, sampling step of 2 cm, cross adit 22, Osnovnoi drift, adit 47, Dzhimi deposit). The bulk metal contents in the apophysis are as follows: 8.7 Fe, 17.6 Zn, 0.5 Pb, and 0.11 wt % Cu (table) and, in recalculation to sulfides, 18.5 FeS_2 , 26.3 ZnS, 0.6 PbS, and 0.3 wt % CuFeS_2 . As compared to the Tsentral'naya vein, Zn contents remain practically the same, but the Fe and Cu contents are two times lower and the Pb content is ten times lower. This indicates that the apophysis was formed within a short time interval: starting at the early pyrite stage to the peak of sphalerite ore formation. In this case, samples with the highest sphalerite contents must be described by the mineral assemblage of layers (8) 9–11. These are data on 2 to 4-cm sampling with the following composition: 17.2 FeS_2 (with allowance for partial Fe incorporation in sphalerite, this value decreases to 10%), 61.5 ZnS, 0.6 PbS, and 0.3–0.5 wt % CuFeS_2 . Evidently, the contents of all minerals coincide with those simulated for the quartz–sphalerite time interval described for the Tsentral'naya vein. However, the apophysis also reveals the partial superposition of mineral assemblages. Its structure suggests that precipitation began with the pyrite assemblage, which was followed by the deposition of the bulk of sphalerite along permeable zones on both sides of the pyrite core. Data on the same apophysis (table) but at a distance of ~20 m from described section also confirm these conclusions.

Data on the Malaya vein (sampling of year 2003, step 3 cm, drift along the Malaya vein, Arkhon gallery, Arkhon deposit; Fig. 15 and table) suggest different conditions of ore formation. The following relations can be distinguished in the distribution of the main four elements: (1) the maximums in the central part of the vein (6–21 cm) are separated in the sequence Fe, Zn, Pb, Cu; (2), the maximum contents decrease from Fe to Cu: the Fe content is more than three times higher than that of Zn or Pb (28.6% against 7.2 and 5.2%, respectively), the maximums of Zn and Pb are close, while the Cu content (0.7%) is ten times lower than those of Zn or Pb; (3) the bulk contents of the main elements decrease from Fe to Cu: 16.4 Fe, 4.5 Pb, 4.1 Zn, and 0.16 wt % Cu.

The former two tendencies are observed only in the central part of the vein, which can be explained as follows: The morphology of the vein indicates that the ore matter precipitated in two time intervals. The first interval involved the formation of the primary vein and the precipitation of sulfides, which was completed by the formation of monolithic gangue quartz. The primary vein is represented by samples from intervals 0–6 cm and, partially, 6–9 cm, as well as the near-contact part (21–24 cm). Upon the completion of its formation and consolidation, the vein was cut by a shear fracture. The earlier material was brecciated, as can be definitely seen in fragments of quartz and even host rocks in the interval of 0–6 cm. The shear fracture unequally cuts the vein into two parts: the larger part is represented by the samples of the interval 0–6 cm, while the smaller part corresponds to the sample of the interval 21–24 cm. During the second time interval (the completion of ore process), the hydrothermal solution partially reworks the primary minerals, while fragments of the brecciation zone are cemented by sulfides and gangue minerals. New mineral formation began at the level of 6–9 cm and was terminated with the formation of monolithic quartz at the interval of 18–21 cm.

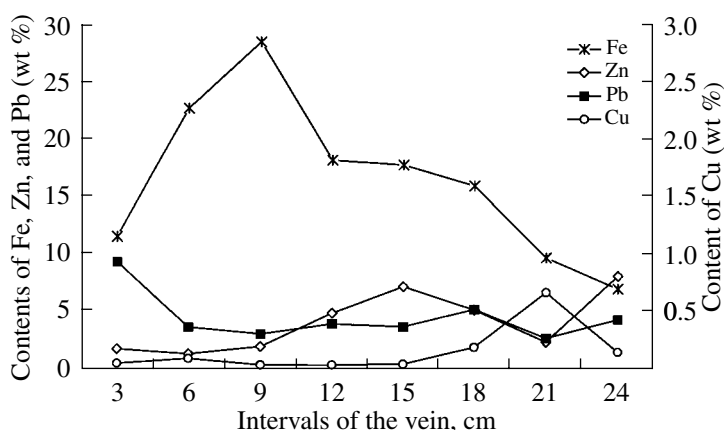


Fig. 15. Distribution of Fe, Zn, Pb, and Cu along the cross section of the Malaya vein (sampling site of 3 cm).

Thus, the tendencies revealed in the distribution of Fe, Zn, Pb, and Cu correspond to the second time interval of the evolution of the Malaya vein. In contrast to the veins considered previously, this one is characterized by lower bulk contents of Zn and distinct differentiation in the precipitation of minerals throughout the section. This distribution of the maximum contents of iron sulfides, sphalerite, galena, and chalcopyrite is often observed in vein bodies at the Sadon district (for example, at the Gatsirovskie and Vostochnaya veins, which were examined at level 6 of the Zgid deposit). However, only the Malaya vein was thoroughly sampled across a detailed cross section.

The recalculation of the bulk Fe, Zn, Pb, and Cu contents to sulfides yields 34.5 FeS₂, 6.1 ZnS, 5.2 PbS, and 0.45 wt % CuFeS₂.⁸ Some of our models of ore formation are well consistent with natural data. The best agreement was obtained in the model with starting conditions in the mobilization zone of 370°C and 600 bar (Fig. 5). This model at 200–240°C (level updip the vein) and 12–15W (“time” interval) contains 20–36.7 FeS₂, 0–4 FeS, 3.7–7.7 ZnS, 0.7–5.6 PbS, and 0.1–0.4 wt % CuFeS₂ (and possibly up to 0.3–0.9% bornite). These bulk contents satisfactorily describe the factual data. The agreement is worse outside the region of these *T* and *W* parameters. Thus, at lower temperatures and/or smaller numbers of waves, the bulk sphalerite contents increase to 11% and more. At higher *T* and *W* values, the amounts of pyrite, galena, and sphalerite diminish.

The model vein at 240°C and 12–15W has the following composition: 40% pyrrhotite and 5.2% sphalerite in layer 0, about 61% pyrite and 0.05% chalcopyrite in layers 1–3, up to 26–28% sphalerite and 0.5% chalcopyrite in layers 4–5, 0.2–8.2% galena and up to 4% galena in layers 6–9, up to 3.7% bornite in layer 10, and so on. This mineral distribution generally corresponds

to those across the Malay vein: 60.9% FeS₂ at the interval of 6–9 cm (without separation between pyrite and pyrrhotite, which is abundant in the natural vein), 10.2% ZnS at the interval of 12–15 cm, 6.0% PbS at 15–18 cm, 2.0 wt % CuFeS₂ (or up to 1.2% bornite) at 18–21 cm. The simulations for sphalerite and Cu minerals yield overestimated values. This can be explained by the contamination of the samples by the material of adjacent intervals (this may cause both under- and overestimations) and different conditions in the mobilization zone (700–900 bar instead of 600 bar; 380°C instead of 370°C). Our aim was to demonstrate that the mineral assemblages of the natural veins are separated in space and quantitatively described by considered models.

In the diagram generalizing our studies (Fig. 10), the field of *T-P* conditions during the mobilization of ore components is divisible into two areas, with each of them having a different structure.

The first, low temperature–high pressure area, is located below the line of the rock/water ratio for elevated background Zn contents (f_2). At such starting conditions, veins are formed with “layers” or practically monomineral sphalerite (the appearance of the quartz–sphalerite time interval). A decrease in the Zn contents in the host granites (from f_2 to f_0) leads to the shortening of the *T-P* range. The temperature decrease with increasing pressure (orthogonally to lines f_2-f_0) within this field gives way to the formation of Zn ores of increasingly lower grades.

The narrow interval of the most favorable conditions for generation of ore-bearing solutions producing rich Zn ores is shown in the diagram by a gray color and occupies the upper part of the first area (Fig. 10). The ore veins simulated under such conditions has a bulk sphalerite content of 30% or more and contains a practically monomineral sphalerite layer (ZnS = 70% and more). The near-contact zones of this vein are composed of the quartz–pyrite assemblage with sphalerite (sphalerite up to 20–30%) overprinted by the quartz–

⁸ The calculations were conducted ignoring that iron is partially incorporated in pyrrhotite, whose early aggregates occur in the vein, as well as in sphalerite and chalcopyrite.

sphalerite assemblage (Fig. 12). Apophyses can be made up of mineralization of any time interval, including quartz–sphalerite, when the high-Zn auxiliary orebodies are formed (for example, the aforementioned Zapadnye apophyses of the Bozang ore zone).

The second, high-temperature–low pressure field is situated above the line f_2 for the water/rock ratios (the area is widened at decreasing background Zn contents in the host granites). These initial conditions ensure the formation of veins without monomineral sphalerite “layers or bands”. The near-contact parts of these veins are enriched in sphalerite, which precipitated along with pyrite and subordinate quartz (Fig. 9). The veins can have a fairly high sphalerite content (more than 30%), but this interval is changed by monomineral pyrite deposition (without sphalerite). Zn-rich orebodies could also be formed under these conditions but during a very brief time period of the evolution of the hydrothermal system. However, apophyses with predominant sphalerite mineralization could not be formed under such conditions.

The applied aspect of our study is as follows. The simulation results indicate a sharp decrease in the Zn and Pb contents with depth. This is seen in all figures, which demonstrate the distribution of the bulk contents of ore minerals with depth (with temperature increase). For example, as is seen in the left-hand part of Fig. 12 for 15W, the sphalerite content shows a 4–5 times decrease when the temperature decreases from 180–200°C (about 25% ZnS) to 250–260°C (up to 5–6% ZnS), with galena disappearing almost completely even earlier. At a vertical paleogradient of 30–40°C/100m [9, 10], a change in the ore formation temperature from 190°C to 250°C should correspond to a depth of 150–200 m down dip the orebody (from sampling site in adit 47). This estimation is close to the depth of productive mineralization inferred by GRP Tsvetmetrazvedka, Vladikavkaz (personal communication).

This publication presents an the equilibrium–dynamic models that quantitatively describes the complete cycle of the evolution of a hydrothermal system from the mobilization zone of ore components to the areas of generation of base-metal veins, which are in a good agreement with data on natural veins. However, there are some constrains, unaccounted factors and parameters that may affect the simulation results. Let us consider some of them.

Levels up dip the vein in our models were isothermal, which is not evident for the natural settings of ore formation. In natural veins, the temperature of mineral formation at a certain level can both decrease and increase up dip the vein. This can be caused by the gradual cooling of the thermal source or drastic changes owing to tectonic motions and the injection of new solution portions. Such models have to be developed.

The assumed structure of the model of ore formation in the vein (temperature step is 10°C, constant pressure, and layer mechanism of mineral precipitation) is only

one of the possible variants. The temperature gradient used therein is justified by data on fluid inclusions, whereas a constant pressure is unlikely. However, estimations made at variable pressure (step 10°C was accompanied by a 50 bar pressure change) showed [5–6, 12] that the pressure gradient in the ore precipitation zone exerts an insignificant effect and can be ignored. The mechanism of reaction–layer ore formation probably fairly often occurs in nature, but its utilization in extensive calculations is not efficient because of the fairly complex processing of simulated data. At a small amount of the matter interacting with new portions of the solution, such models yield results close to the pure layer mechanism but show a decrease in the maximum contents of ore elements and the partial overlapping of their local crystallization in the sections of model veins [13].

The simulated results strongly depend on the input thermodynamic information. Our data are well consistent with experimental data on the solubility of sphalerite and other sulfides [17] (experiments were conducted in the system synthetic quartz–muscovite–K-feldspar buffer in the presence of pyrite–pyrrhotite–magnetite–sphalerite–galena–chalcopyrite and without exchange with the solution). In particular, the average Zn contents were 11.4×10^{-3} m in experiments at 350°C and 1 kbar and $5.1\text{--}8.2 \times 10^{-3}$ at 400°C and 1 kbar. Our calculations for the mobilization zone showed that the Zn content at 360°C and 1 kbar was 1.4×10^{-3} (extreme solubility) and from 5.1×10^{-3} to 9.5×10^{-3} m at 400–410°C and 1 kbar. This agreement highlights the high plausibility of our calculations.

The composition of the primary barren solution was assumed constant in this research but it can be varied. We touched upon this problem in our previous papers [5–6, 12, 14], in which models of mobilization and ore formation were analyzed at wide variations in primary solution composition (H_2CO_3 0–0.5 m; NaHCO_3 0–0.7 m; NaCl 0.4–1.0 m; KCl 0–0.2 m, CaCl_2 0–0.3 m, HCl 0–0.1 m, and H_2S 0–0.001 m). We established the limiting concentrations of Na and NaHCO_3 at which unrealistic mineral assemblages of the metasomatites were formed near the mobilization zones (an increase in the albite content) and determined the solution compositions that change the sequence of the complete leaching of Pb and Cu. However, compositional variations in the solution at a constant total Cl content of 1 m do not lead to significant changes in the solubility of sphalerite and other sulfides.

The second factor in the mobilization zone is the host rock, whose major- and trace-element compositions can vary. In this publication, a bulk major-element composition of the Sadon granite was taken as that of the starting rock. In [5–6, 14], simulation was performed with another granite composition. It was found that the mobilization of ore components is most strongly affected by the content of sulfide sulfur and the Fe(II)/Fe(III) ratio. An increase in the sulfide sulfur concentration in the rock to 0.1 wt % and more could

lead to a decrease in the solubility of sulfides of ore elements and the prolongation of their leaching, but the main tendencies in ore formation remain the same, as was described above. Insignificant variations in the contents of major elements (Si, Al, Na, K, Ca, and Mg) typically do not lead to any principal changes and exert practically no effect on ore formation.

Much attention was focused in our research on Zn and the influence of its background contents in the host granites on ore formation. Practically no attention was paid to the variations in Pb and Cu contents. However, by analogy with Zn, a change in the contents of these elements should probably also affect the character and quantitative characteristics of mineral formation in the veins. This problem can, however, be solved by specialized geochemical investigations and thermodynamic simulations.

CONCLUSIONS

1. Prolonged interaction in the system barren hydrothermal solution–host rock leads to the formation of ore-bearing solutions with variable metal contents. It was established that the parameters of the hydrothermal system in the mobilization zone are correlated with the formation of the characteristic geochemical structure and mineral assemblages of natural veins.

2. Our simulation results show that filling veins with bulk sphalerite content of ~30% and its practically monomineral “layers” in cross-sections can be formed from ore-bearing solutions within a narrow range of conditions in the metal mobilization zone: 410–440°C and 900–1200 bar, granite with elevated background contents of Zn (≥ 0.007 wt %). This maximum Zn contents (both bulk and local contents up dip the vein) are reached within the temperature range of 150–200°C.

ACKNOWLEDGMENTS

We are grateful to K.V. Davydov and S.B. Lyasovskii, GRP Tsvetmetrazvedka (Vladikavkaz), for the useful discussion of our preliminary results and help in the work at the Dzhimi deposit. We also thank D.V. Grichuk and Vikt.L. Barsukov for useful comments during manuscript preparation and R.A. Mitoyan, I.P. Rodionova, V.A. Buguliev, M.M. Zuntov, and E.V. Konina. This study was supported by the Russian Foundation for Basic Research (project no. 05-05-64223), Federal Program for the Support of the Leading Scientific Schools (project no. NSh-491.2003.5), and the Program “Russian Universities” (project no. UR-09-03-003).

REFERENCES

1. G. V. Khetagurov, L. V. Shchepetova, T. V. Vasil'eva, and K. L. Rekhviashvili, *Mineralogical Composition and Distribution of Major and Minor Elements in the Ore Deposits Mined by the Sadon Combine. Report* (Sev.-Kavk. Gornometallurg. Inst., Ordzhonikidze, 1992) [in Russian].
2. V. I. Smirnov, *The Geology of Mineral Deposits* (Nedra, Moscow, 1976) [in Russian].
3. E. M. Nekrasov, *Structural Environments for Localization of Vein Lead–Zinc Deposits* (Nedra, Moscow, 1980) [in Russian].
4. M. V. Borisov, “Regularities in the Distribution of Elements in Wall Rocks at Vein-hosted Pb–Zn Hydrothermal Deposits,” *Geokhimiya*, No. 11, 1115–1127 (1997) [*Geochem. Int.* **35**, 985–996 (1997)].
5. M. V. Borisov, *Geochemical and Thermodynamic Models of the Formation of Vein Hydrothermal Ore Mineralization* (Nauchnyi Mir, Moscow, 2000) [in Russian].
6. M. V. Borisov, “Geochemical and Thermodynamic Models for the Genesis of Low- and Medium-Temperature Vein Mineralization and Metasomatism in the Wall Rocks,” *Geochem. Int.* **41** (Suppl. 2), 145–312 (2003).
7. B. G. Amov, Z. V. Otkhmezuri, and Ts. T. Baldzhieva, “Ore Sources at Some Base-Metal Deposits of the Great Caucasus in the Light of the Pb Isotopic Composition,” *Zap. Vses. Miner. Obshchestva*, No. 5, 595–601 (1988).
8. K. L. Rekhviashvili, G. V. Khetagurov, A. V. Darchieva, et al., “Redistribution of Elements in the Wall Rocks of Postmagmatic Deposits as Exemplified by the Sadon Ore District,” *Zap. Vses. Mineral. O-va* **119**, 63–75 (1990).
9. E. M. Laz'ko, Yu. V. Lyakhov, and A. V. Piznyur, *Physicochemical Principles in Predicting Postmagmatic Mineralization* (Nedra, Moscow, 1981) [in Russian].
10. Yu. V. Lyakhov, K. M. Pozdeev, S. M. Tibilov, et al., “Model of Ore Zoning at the Sadon Lead–Zinc District Based on Data on Fluid Inclusions and Assayed Outlooks of the District,” *Rudy Met.*, No. 2, 45–54 (1994).
11. M. V. Borisov and K. Yu. Kudryavtsev, “Thermodynamic Models of the Ore Body Formation at Veined Lead–Zinc Deposits,” *Dokl. Earth Sci.* **368**, 943–945 (1999) [*Dokl. Akad. Nauk* **368**, 87–90 (1999)].
12. M. V. Borisov, “Thermodynamic Models for Deposition of Pb–Zn Veins,” *Geokhimiya*, No. 8, 829–851 (2000) [*Geochem. Int.* **38**, 750–771 (2000)].
13. M. V. Borisov, D. A. Bychkov, and Yu. V. Shvarov, “Thermodynamic Simulation of the Genesis of Filling Veins,” *Geochemistry International* **40** (Suppl. 1), 92–102 (2002).
14. M. V. Borisov and Yu. V. Shvarov, “Mobilization of Ore Components during the Formation of Pb–Zn Hydrothermal Lodes: A Thermodynamic Model,” *Geokhimiya*, No. 2, 166–183 (1998) [*Geochem. Int.* **36**, 134–149 (1998)].
15. Yu. V. Shvarov, “Algorithmization of the Numeric Equilibrium Modeling of Dynamic Geochemical Processes,” *Geokhimiya*, No. 6, 646–652 (1999) [*Geochem. Int.* **37**, 571–576 (1999)].
16. Yu. V. Shvarov and E. N. Bastrakov, *HCh: a Software Package for Geochemical Equilibrium Modelling (User's Guide)* (Austral. Geol. Surv., Canberra, 1999).
17. J. J. Hemley, G. L. Cygan, G. B. Robinson, and W. M. D'Angelo, “Hydrothermal Ore-Forming Processes in the Light of Studies in Rock-Buffered Systems. I. Iron–Copper–Zinc–Lead Sulfide Solubility Relations,” *Econ. Geol.* **87**, 1–22 (1992).